

**DEVELOPMENT OF ELECTROMAGNETIC TRANSPORT  
MEASUREMENT SYSTEM FOR SPINTRONICS APPLICATION**

**A  
PROJECT REPORT  
*Submitted by***

**DAVID JOYSON  
NAMITA THYKKAT  
SOWJANYA K**

(15030141ECE015)  
(15030141ECE033)  
(15030141ECE051)

*In partial fulfillment for the award of the degree of*

**BACHELOR OF TECHNOLOGY  
IN  
ELECTRONICS AND COMMUNICATION ENGINEERING**

**Under the guidance of**

**Dr. Harinath Aireddy**



**Department of Electronics and Communication Engineering  
ALLIANCE COLLEGE OF ENGINEERING AND DESIGN**

**Chikkahagade Cross  
Chandapura-Anekal Main Road  
Bangalore-562106**

**MAY- 2019**

# **Department of Electronics and Communication Engineering**

**Alliance College of Engineering and Design,  
Alliance University  
Chikkahagade Cross  
Chandapura-Anekal Main Road,  
Bangalore-562106.**



## **CERTIFICATE**

This is to certify that the project work entitled "**Development Of Electromagnetic Transport Measurement System For Spintronics Application**" is the bonafide work done by **Mr. David Joyson** (15030141ECE015) , **Ms. Namita Thykkat** (15030141ECE033) and **Ms. Sowjanya K** (15030141ECE051) submitted in partial fulfilment of the requirements for the award of the degree **Bachelor of Technology in Electronics and Communications** during the year **2018-2019**.

**Dr. Harinath Aireddy**  
Supervisor

**Dr. Chitra Kiran**  
Head of Department

**External Examiners:** 1. Name: \_\_\_\_\_ Signature: \_\_\_\_\_  
2. Name: \_\_\_\_\_ Signature: \_\_\_\_\_



## DECLARATION

This is to declare that the report titled "**“Development Of Electromagnetic Transport Measurement System For Spintronics Application”**" has been made for the partial fulfillment of the Course Bachelor of Technology in Electronics and Communication Engineering, under the guidance of **Dr. Harinath Aireddy**.

We confirm that this report truly represents our work undertaken as a part of our project work. This work is not a replication of work done previously by any other person. We also confirm that the contents of the report and the views contained therein have been discussed and deliberated with the faculty guide.

NAME	REG NO.	SIGNATURE
DAVID JOYSON	15030141ECE015	
NAMITA THYKKAT	15030141ECE033	
SOWJANYA K	15030141ECE051	

## **ACKNOWLEDGEMENT**

The satisfaction that accompanies the successful completion of the task would be put incomplete without the mention of the people who made it possible, whose constant guidance and encouragement crown all the efforts with success. We are very thankful to our guide **Dr. Harinath Aireddy**, Department of Electronics and Communication Engineering for his sustained inspiring guidance and cooperation throughout the process of this project. His wise counsel and valuable suggestions are invaluable.

We would like to thank **Dr. Chitra Kiran**, Head of the department for her encouragement and cooperation at various levels of Project.

We would like to thank **Prof. T. Sridhar**, Project coordinator for his valuable suggestions and **Dr. Reeba Korah**, Associate Dean, ACED for her constant support and encouragement.

We would like to express our deep gratitude to **Prof. Rohan Veigas**, Department of Mechanical Engineering for guidance and constant support.

We avail this opportunity to express our deep sense of gratitude and hearty thanks to the **Management of Alliance University**, for providing world class infrastructure, congenial atmosphere and encouragement.

We express our deep sense of gratitude and thanks to the teaching and non-teaching staff at our department who stood with us during the project and helped us to make it a successful venture.

We place highest regards to our parents, my friends and well-wishers who helped a lot in making the report of this project.

**DAVID JOYSON**

**NAMITA THYKKAT**

**SOWJANYA K**

## **ABSTRACT**

The development in the field of electronics has grown vast in the past few decades. Conventional electronic devices rely on the transport of electric charge carriers-electrons-in a semiconductor such as silicon device. As the Moore law gradually loses its effect, conventional charge-based electronics is coming to an end as we have reached to a nanoscale size of components and further reduction in size would affect the functioning of the device due to quantum effects. Today engineers and physicists are trying to exploit the spin of an electron than charge which gives rise to an new emerging and promising field called Spintronics which uses the spins of electrons as information carriers and possesses potential advantages of speeding up data processing, high circuit integration density, and low energy consumption. The key property in Spintronics is the measurement of magnetoresistance i.e. the electrical resistance under the influence of magnetic field and this magnetoresistance can be measured using a transport measurement system which is the goal of our project. We have designed and fabricated a electromagnetic transport measurement system that is compact, automated and low cost. A thin film of Fe<sub>3</sub>O<sub>4</sub> is deposited onto the silicon substrate by using Pulsed laser Deposition(PLD) process for injection of spin onto a semiconductor. The fabricated heterostructure is placed on the sample holder which is automated by a robotic arm that is powered up using Arduino for the rotation of in plane, out-of plane and anisotropic measurements. By two probe method, voltage is supplied to the sample and the current value is measured and thereby magnetoresistance is calculated from the slope of I-V characteristics which gives us the behaviour of the sample for spintronics application. Multiple samples can be loaded onto this system and magnetoresistance can be measured which will enable a fundamental understanding of new effects emerging in the field of spintronics.

**Keywords:** Transport measurement system, Magnetoresistance, Robotic arm, Arduino, Heterostructure, spin-injection, pulsed laser deposition, two-probe method

## CHAPTER 1

### INTRODUCTION

#### 1.1. PREAMBLE

The transistor is the fundamental block of modern semiconductor-based electronic devices. The field of electronics has developed very quickly past few decades giving rise to microelectronics and fabrication of microchips that follows the fundamentals of Moore's Law. Moore's Law summarizes the continuous growth of microelectronics, which states that the transistor density on a chip is doubled in every 18 months. Heat generation and increasing power consumption rate limit the operating speed of semiconductor integrated circuits to below the individual transistors capabilities. Scaling limit and extraordinary challenges in silicon-based transistors are expected to end the silicon road map. So, there is a clear need to explore alternatives that can extend or even replace the existing semiconductor technology. One of the emerging and most promising field is the semiconductor-based Spintronics which rely on the spin of the electron as functional unit rather than charge of an electron. The spin of an electron is purely a quantum mechanical concept and described as either spin-up( $+1/2$ ) or spin-down( $-1/2$ ); which therefore can lead to an entirely new logic concept very much alike to charge based "0" and "1" digital states. Another most important property of an electron spin is its long coherence or relaxation time, which will step up the possibility of making use of the electrons charge and spin to achieve powerful spin-based electronic devices which would be smaller in size, non-volatile in nature, faster in computation and less power consumption when compared with the only charge based electronic devices.

## 1.2. BACKGROUND

Information technology is one of the important issues in the 21st century. As the Moore law gradually loses its effect, conventional charge-based electronics will come to the end in the near future. Developing alternative high speed and low energy consuming information technology is urgently needed. Up to now, many new methodologies have been proposed, such as molecular electronics, nanoelectronics, spintronics, and quantum information techniques, among which spintronics is one of the most promising ones. Compared to other methodologies, spintronics is compatible with conventional electronics, thus many techniques used in conventional electronics can be directly extended to spintronics[1]. Spintronics refers commonly to a phenomena in which the spin of the electrons in solid state environment plays the determining role. Spin devices are based on spin control of electrons or on an electrical or optical control of spin or magnetism [2].

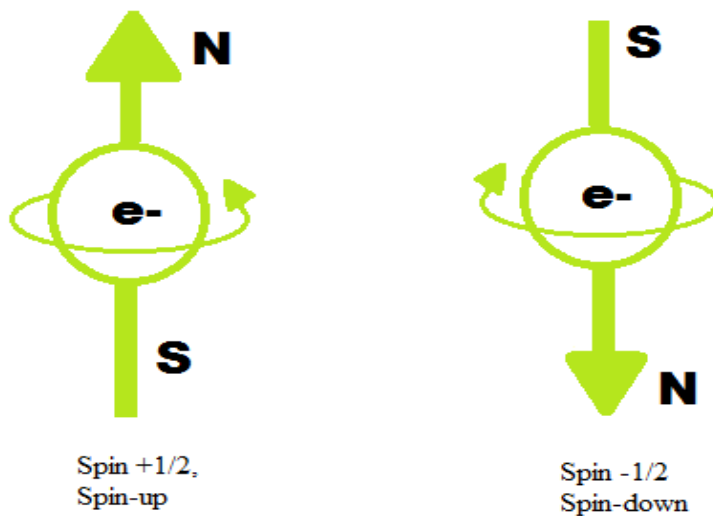


**Figure 1:** Spin states of an electron in Spintronics

Spintronics emerged from discoveries in the 1980s concerning spin-dependent electron transport phenomena in solid-state devices. This includes the observation of spin-polarized electron injection from a ferromagnetic metal to a normal metal(1985), and the discovery of

giant magneto resistance(1988). The discovery of giant magnetoresistance (GMR) is regarded as the beginning of spintronics[1]. From last two decades, development of spintronics has both an extremely fruitful direction of research into the properties and usefulness of the spin degree of freedom of the electron as it can apply to the exponentially expanding world of electronics. Spintronics has infiltrated almost every household in the form of the read head sensors for the hard drives that inhabit every desktop and most laptop computers[3]. Different from conventional electronics, which uses the electron's charge degree of freedom for information processing, spintronics is devoted to incorporating the electron's spin degree of freedom. In an ideal situation, there will be purely spin current and no charge current in the spintronic circuit, thus no heat will be created and wasted. Meanwhile, information will be transmitted at a high speed owing to the spin coherence effect [1].

The central aspiration of spintronics is to utilize the spin degree of freedom of carriers in semiconductors along with the conventional charge degree of freedom to enhance the functionality of semiconductor-based electronics. The spin-based technology is expected to have a thoughtful influence on data storage, logic gates, and self-memory of electronic devices. Spin-polarized tunneling through a thin tunnel barrier is a more practical approach to inject spin polarized carriers from ferromagnetic (FM) materials into semiconductors and has been demonstrated for the injection and detection of spin polarized carriers in GaAs and Si . Several groups have investigated the transport properties of ferromagnet/semiconductor heterostructures taking different ferromagnets like dilute magnetic semiconductors (DMSs), transition metals , magnetites , etc and have discovered new magnetically tunable magnetoresistance (MR) properties. The Magnetoresistance (MR) observed in the above heterojunctions has been correlated with the Zeeman splitting effect , magnetic-field controlled avalanche breakdown and minority spin carrier related transport . However, most of the reported MR occurs only at a higher magnetic field , higher bias voltage or at lower temperatures, which limits their device applications. Evidently, beneficial spin transport electronic devices like spin valves, spin filters , spin transistors , and tunneling based magnetoresistive elements require FM materials with large spin polarization and a high Curie temperature (Tc) [4].

Spin can be visualised as the Earth turning on its own axis while rotating around the sun. In the same way, an electron spins on its own axis while rotating around an atom's nucleus. Spin is either "up" or "down". In the same way traditional electronics uses charge to represent information as zeros and ones, the two spin states can be used to represent the same binary data in spintronics. Spin can be measured because it generates tiny magnetic fields. Ferrous metals such as iron become magnetic, for example, when enough particles have their spin set in the same direction, generating a magnetic field of the same polarity as the spin.

Spintronics has several advantages over conventional electronics. Electronics require specialised semiconductor materials in order to control the flow of charge through the transistors. But spin can be measured very simply in common metals such as copper or aluminium. Less energy is needed to change spin than to generate a current to maintain electron charges in a device, so spintronics devices use less power. Spin states can be set quickly, which makes transferring data quicker. And because electron spin is not energy-dependent, spin is non-volatile – information sent using spin remains fixed even after loss of power [5].

Spintronics can be used in variety of application like Spintronics Devices (includes spin-based transistor), Information Storage Devices(magnetic tape, floppy disk), Spin Valve (device consisting of two or more conducting magnetic materials), Quantum Electromagnets (electromagnets are wire coils or loops), Microelectronic Devices (MOSFETS, Bipolar Transistor), Sensors (measures a physical quantity and converts it into a signal which can be ready by an instrument), Spintronic Scanner for Cancer Detection etc [6].

Despite its great potential advantages, spintronics now faces a number of challenges, such as generation of fully spin-polarized carriers (pure spins) and injection of spin into devices, long distance spin transport, and manipulation and detection of carriers' spin orientation. The solutions to these issues rely on the development of device fabrication and optimization techniques on one hand, and designing new spintronics materials with specific properties on the other hand. To solve the above issues, diverse spintronics materials have been designed. According to their electronic and magnetic properties, spintronics materials can be classified as magnetic metals, topological insulators (TIs), and magnetic semiconductors.

### **1.2.1. Magnetic metals and TIs**

Magnetic metals and TIs Ferromagnetic metals Ferromagnetic metals include Fe, Co, Ni metals, and also their alloys. They are the oldest spintronics materials that were used to construct spin valves and magnetic tunnel junctions. These materials are abundant and cheap, and can be handled easily. However, they can only supply partially spin-polarized carriers due to their low degree of spin polarization.

### **1.2.2. Topological Insulators**

TIs are a special type of insulators, which are insulating in their bulk but metallic on their surface. Moreover, the metallic surface states are symmetry protected. Interestingly, the spin-up and spin-down electrons propagate in opposite direction on the surface. Thus, TIs are ideal for pure spin generation and transport, without bringing any net charge current. Typical examples of TIs are HgTe and Bi<sub>1-x</sub>Sbx. All TIs realized so far can only work at low temperatures, and still have a long way to go before their practical applications.

### **1.2.3. Magnetic Semiconductors**

Magnetic semiconductors, combining the properties and advantages of both magnets and semiconductors, form the basis for spintronics. Magnetic semiconductors can be applied for spin generation and injection, and spin manipulation and detection. Compared to other spintronics materials, magnetic semiconductors can be easily implemented in devices by utilizing nowadays well-developed semiconductor technology. Unfortunately, most magnetic semiconductors suffer from low magnetic ordering temperatures, hindering their practical applications. In general, magnetic semiconductors can be divided into two categories: diluted magnetic semiconductors (DMSs) and intrinsic magnetic semiconductors. Furthermore, based on different electronic and magnetic properties, intrinsic magnetic semiconductors can be subdivided into half semiconductors (HSCs), spin gapless semiconductors (SGSs), bipolar magnetic semiconductors (BMSs), and asymmetric antiferromagnetic semiconductors (AAFMSs)[1]. Worldwide efforts are underway to integrate semiconductors and magnetic materials, aiming to create a revolutionary and energy-efficient information technology in which

digital data are encoded in the spin of electrons. Implementing spin functionality in silicon, the mainstream semiconductor, is vital to establish a spin-based electronics with potential to change information technology beyond imagination[2]. The highly used semiconductor is silicon wafer. Silicon is preferred over other semiconductors due long spin lifetime and easy to manufacture at large scale production.. To successfully incorporate spins into existing semiconductor technology, one has to resolve technical issues such as efficient injection, transport, control and manipulation, and detection of spin polarization as well as spin polarized currents. Semiconductor spintronics combine the advantage of semiconductor with the concept of magnetoelectronics. This category of devices include spin diodes, spin filter, and spin Field Effect Transistor. To make semiconductor based spintronic devices, several problems need to be addressed. First problem is creation in inhomogeneous spin distribution. it is also called as spin polarization or spin-injection. Second problem is achieving transport of spin-polarized electrons maintaining their spin orientation. The field of spintronics is young and difficult to predict how it will evolve. New physics is being discovered and new materials are being developed such as magnetic semiconductors and exotic oxides that manifest even more extreme effects. To study and analyze the material, one need to understand and measure the magnetoresistance as it is the important property in spintronics[7].

#### **1.2.4. Magnetoresistance**

Giant Magnetoresistance was independently discovered in 1988 in Fe/Cr/Fe trilayers by a research team led by Peter Grunberg, who owns the patent, and in Fe/Cr multilayers by the group of Albert Fert of the University of Paris-Sud, who first saw the large effect in multilayers (up to 50% change in resistance) that led to its naming, and first correctly explained the underlying physics. The discovery of GMR is considered as the birth of Spintronics. Like other magnetoresistive effects, giant magnetoresistance (GMR) is the change in electrical resistance of some materials in response to an applied magnetic field. There are a variety of effects that can be called magnetoresistance. Resistance may depend on magnetic field through various mechanisms, it is useful to separately consider situations where it depends on magnetic field directly. Magnetoresistance will establish the injection of spin in the semiconducting

material[7]. The MR is termed as a JMR which is the total resistance of the given heterostructure, including the junction/interface effect, and defined as,

$$MR \% = \frac{\Delta R}{R} \times 100\% = \frac{(R(B \neq 0)) - (R(B=0))}{(R(B=0))} \times 100\%$$

where,  $\Delta R$  and  $R$  are resistance in magnetic fields of a magnitude  $B$  and zero, respectively, and  $R(B \neq 0)$  and  $R(B=0)$  are similar electrical resistances with and without magnetic field respectively.  $\Delta R/R$  depends on the magnetic field  $B$ , ie, its magnitude and direction as well.

There are various techniques to measure magnetoresistance and one of the simplest method to measure Magnetoresistance is by using a transport measurement system.

#### **1.2.5. Transport Measurement System**

This system makes it possible to measure the electrical transport properties of monocrystals, thin films or magnetic multilayers under magnetic field at specific range of temperature. The availability of transport measurement systems in India are very limited and presently there are no systems that can perform both isotropic and anisotropic measurements of a sample from laboratory point of view.

### **1.3. OBJECTIVE**

The objective of this project is development and implementation of an electromagnetic transport measurement system for spintronics application which will enable a fundamental understanding of new effects emerging in the field of spintronics. The understanding, quantification of these effects will underpin Research & Development and future applications in metrology, Information and Communication Technologies, and other fields. It will also take the first steps towards future standardisation of spintronic measurements, materials, and devices by the development of a new measurement infrastructure and a best practice guide for spintronics material measurements. The following phases need to be completed to meet the objective,

- To design an automated and compact electromagnetic transport measurement system
- To create spin injection in the sample
- To achieve the transport of the spin-polarized electrons maintaining their spin orientation.

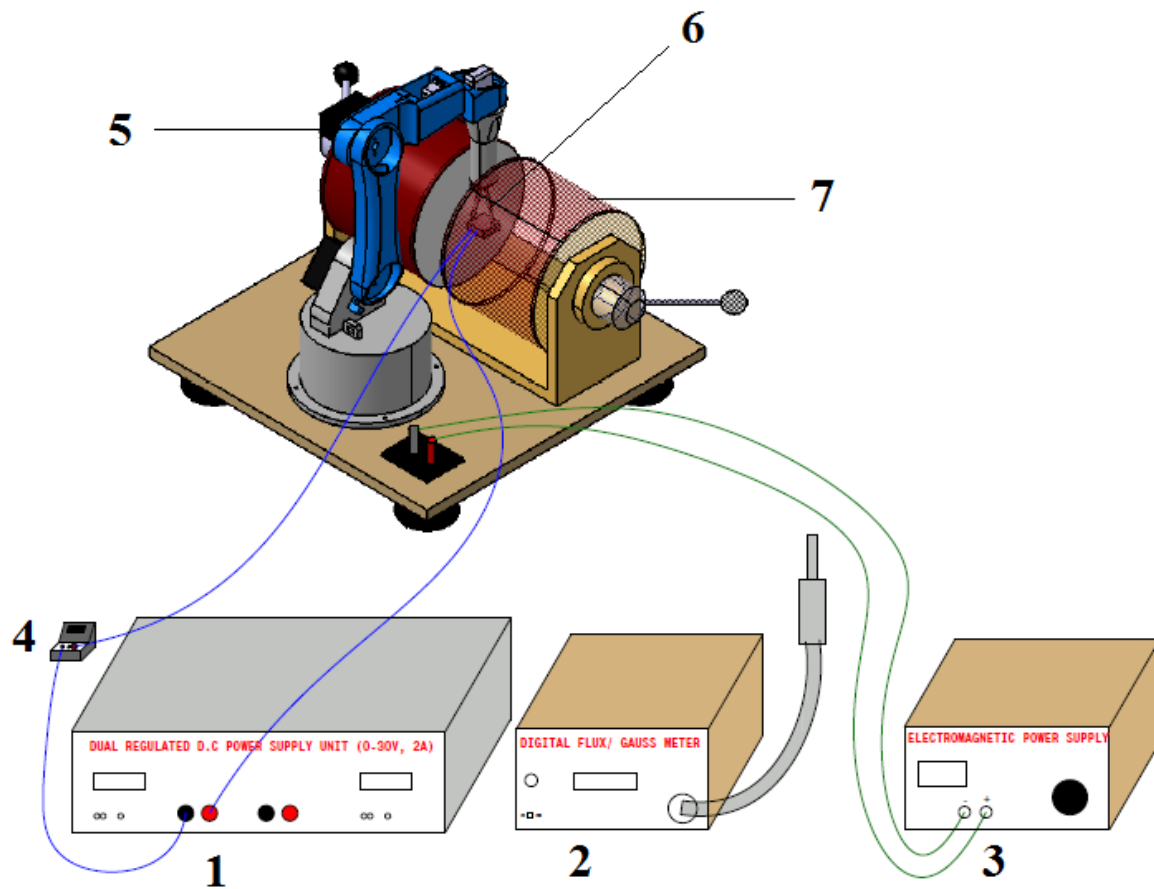
- To measure the magnetoresistance of the given sample
- Simulate design using arduino microcontroller.
- Implement the simulated design along with hardware and software specifications.

## CHAPTER 2

### DESIGN AND DEVELOPMENT OF ELECTROMAGNETIC TRANSPORT MEASUREMENT SYSTEM

#### 2.1. SCHEMATIC DIAGRAM OF TRANSPORT MEASUREMENT SYSTEM

The below fig. 2 shows a schematic view of the electromagnetic transport measurement system. The instruments used to fabricate the system are: a electromagnet to generate magnetic field, a electromagnetic power supply to power up the electromagnet, a gauss meter to measure the magnetic field produced by the electromagnet, a robotic arm which holds the sample and is programmed to rotate in-plane, out-of plane and isotropic, a heterojunction sample Fe3O4/SiO<sub>2</sub>/Si to which a voltage supply is connected and simultaneously current produced is measured on an ammeter.



- 1.Dual regulated DC power supply (0-30V), 2. Gauss meter, 3.Electromagnetic power supply, 4. Ammeter, 5.Robotic arm, 6. Sample, 7. Electromagnet

**Figure 2: Schematic diagram of electromagnetic transport measurement system**

## **2.2. COMPONENT DESCRIPTION AND SPECIFICATION**

### **2.2.1. Electromagnet**

An electromagnet is a type of magnet in which the magnetic field is produced by an electric current. Electromagnets usually consist of wire wound into a coil. A current through the wire creates a magnetic field which is concentrated in the hole in the center of the coil. The magnetic field disappears when the current is turned off. The wire turns are often wound around a magnetic core made from a ferromagnetic or ferrimagnetic material such as iron; the magnetic core concentrates the magnetic flux and makes a more powerful magnet. The main advantage of an electromagnet over a permanent magnet is that the magnetic field can be quickly changed by controlling the amount of electric current in the winding. However, unlike a permanent magnet that needs no power, an electromagnet requires a continuous supply of current to maintain the magnetic field.

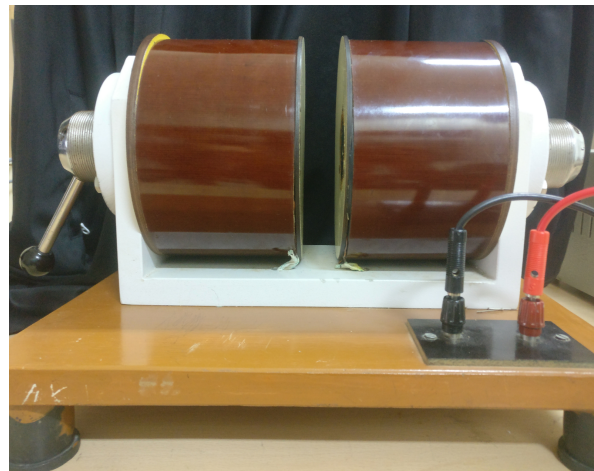


**Figure 3: Image of Adjustable Air Gap Electromagnet**

#### **Specification :**

- Type: Adjustable air gap electromagnet
- Input current range: 0A-5A
- Magnetic field strength: 0T-2T

- Diameter of the pole: 4.7 cm
- Resistance of each coil: 20 ohms
- Total resistance : 10 ohms
- Resistivity of copper:  $1.68 \times 10^{-8}$
- Diameter of wire: 0.1cm

### 2.2.2. Electromagnetic Power Supply

An electromagnet requires a continuous supply of current to maintain the magnetic field unlike permanent magnet. This continuous supply of current is provided by the electromagnetic power supply source.

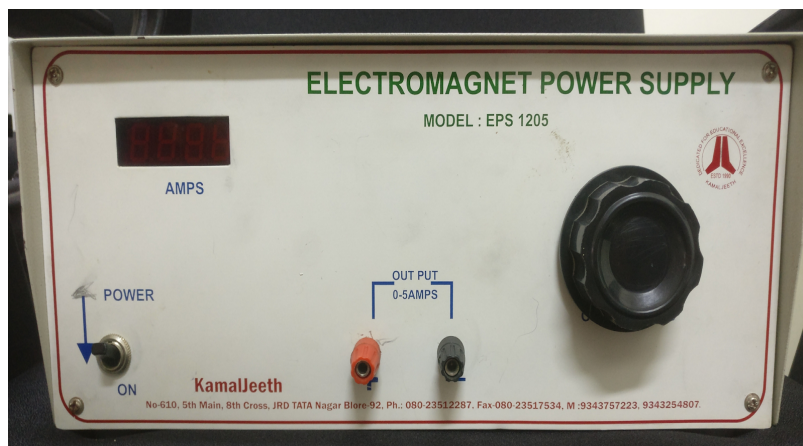


**Figure 4:** Image of Electromagnet Power Supply

#### Specification:

- Type: Electromagnetic power supply
- Output Voltage: 0-70V unregulated
- Output Current: 0-5A
- Voltmeter: 0-200V (Digital)

### 2.2.3. Gauss meter and Gauss probe

A gaussmeter, also known as a magnetometer, is a device used to measure the strength and direction of a magnetic field. It consists of a gauss probe, the meter itself and a cable to connect them. Gauss meter is used to measure relatively small magnetic fields. The connection cable links the gaussmeter to the probe. The gauss sensor is basically a Hall probe, and it's the most

important part of a gauss meter to get a reading. It can be flat, which is best for measuring transverse magnetic fields, or it can be axial, which best measures fields parallel to the probe, such as those that exist inside a solenoid. The meter sends a test current through the probe, and the hall effect produces a voltage which the meter then records .



**Figure 5:** Image of Gauss meter and Gauss probe

#### SPECIFICATION :

- Range: 0 kG- 20 kG

#### 2.2.4. Robotic Arm

A robotic arm is a type of mechanical arm, usually programmable, for desired functions. The links of such a manipulator are connected by joints allowing rotational motion using a servo motor. The arm is 3D printed for the desired specification with 4 axis freedom of movement incorporated by 4 servo motors powered by a arduino board. A control system controls the power supplied to each motor and precise movement of the holder. The main motive of the robotic arm is to attach the sample holder along with the sample. Sample holder is mounted in such a way that the sample held by it is placed in between the electromagnet and automatically rotated in order to measure in-plane, out-plane, isotropic and anisotropic characteristics of that sample. This Automated robotic arm Systems employs 4-axis, in flexible automation on both horizontal and vertical;

- Axis 1(Shoulder servo) - Forward / back extension of sample holder's lower arm
- Axis 2(Elbow servo) - Raises / lowers sample holder's upper arm
- Axis 3(wrist servo) - Raises / lowers wrist of sample holder's arm

- Axis 4 (hand servo)- Rotates wrist of the sample holder's arm



**Figure 6:** Image of Robotic Arm

#### **Specification:**

- Consists of 4 axis and 4 servo motors used.
- Standard voltage for servo motor: 4.8 V (DC)
- Microcontroller: Arduino uno which is connected to a computer system
- Angle of rotation of servo: (0°- 90°)or (90°-180°)or (180°-360°)
- Overall length: 42 cm
- Material of sample holder: copper
- Material of robotic arm: stainless steel

#### **2.2.5. Voltage Source Supply**

The voltage supply source is a device that supplies electrical power to a circuit in the form of a voltage . The voltage is supplied to the sample in steps of 0.1v and corresponding current values are noted down.



**Figure 7:** Image of Dual Regulated Power Supply

#### Specifications:

- Type: Dual regulated dc power supply
- Output Voltage: 0 v- 30 v
- Output Current: 2 A

#### 2.2.6. DC Ammeter

An ammeter is a measuring instrument used to measure the current in a circuit. Electric currents are measured in amperes (A), hence the name. The ideal ammeter has zero internal resistance. But practically the ammeter has small internal resistance. The measuring range of the ammeter depends on the value of resistance.

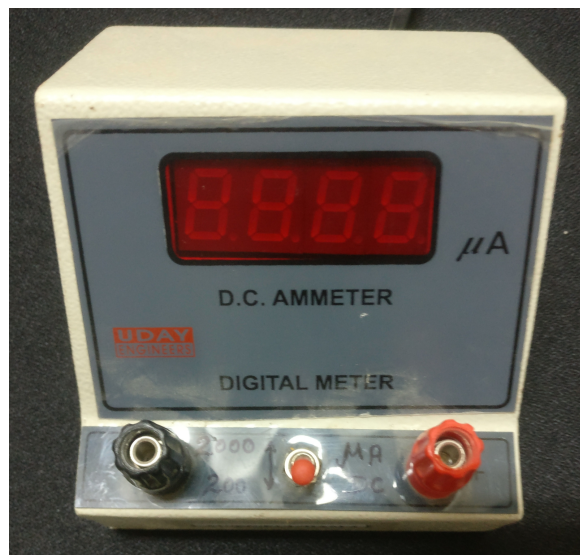


**Figure 8:** Image of DC Ammeter

### **Specifications:**

- Type: DC ammeter
- Range: 0 $\mu$ m-2000 $\mu$ m

### **2.2.7. Arduino UNO**

Arduino Uno board is a microcontroller board based on the ATmega328. It has 14 digital input/output pins, 6 analog inputs, a USB connection, power jack, an in-circuit serial programming (ICSP) header and reset button. It is simply connect to a computer with a USB cable or power it with alternating current (AC)-to- direct current (DC) adapter or battery to get started.

### **Specifications:**

- Microcontroller: Microchip ATmega328P
- Operating Voltage: 5 Volts
- Input Voltage: 7 to 20 Volts
- Digital I/O Pins: 14 (of which 6 provide PWM output)
- Analog Input Pins: 6
- DC Current per I/O Pin: 20 mA
- DC Current for 3.3V Pin: 50 mA
- Flash Memory: 32 KB of which 0.5 KB used by bootloader
- SRAM: 2 KB
- EEPROM: 1 KB
- Clock Speed: 16 MHz
- Length: 68.6 mm
- Width: 53.4 mm
- Weight: 25 g

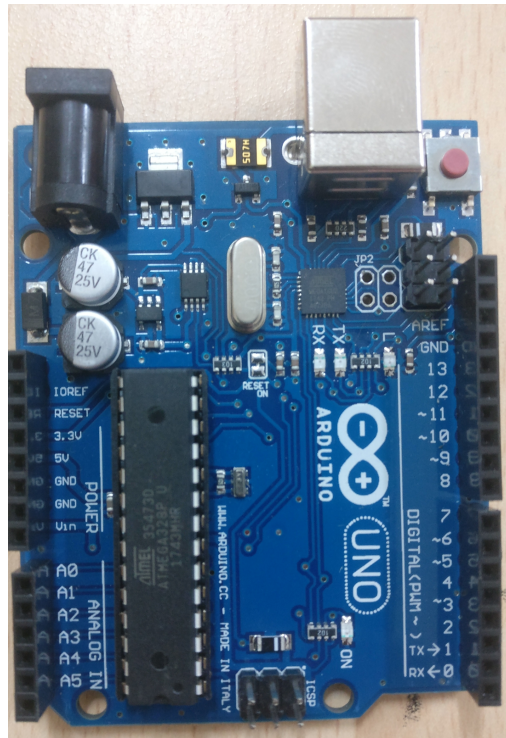


**Figure 9:** Image of Arduino uno board

## 2.3. DESIGN OF ROBOTIC ARM

### 2.3.1 Schematic Diagram of Robotic Arm

The mechanical design of the robotic arm is done to meet our instrument specifications. The below figure 9 shows detailed dimensions of the fabricated robotic arm which consists of a base, waist, shoulder, elbow, wrist roll, wrist and a sample holder. The base of the robotic arm is tightly screwed on to the table for a stable movement of the arm. Shoulder and elbow of robotic arm is programmed to rotate 180 degree. Wrist roll is connected to the wrist where a sample holder is attached, the wrist roll servo motor rotates the wrist as well as sample holder from 0 degree to 180 degree.

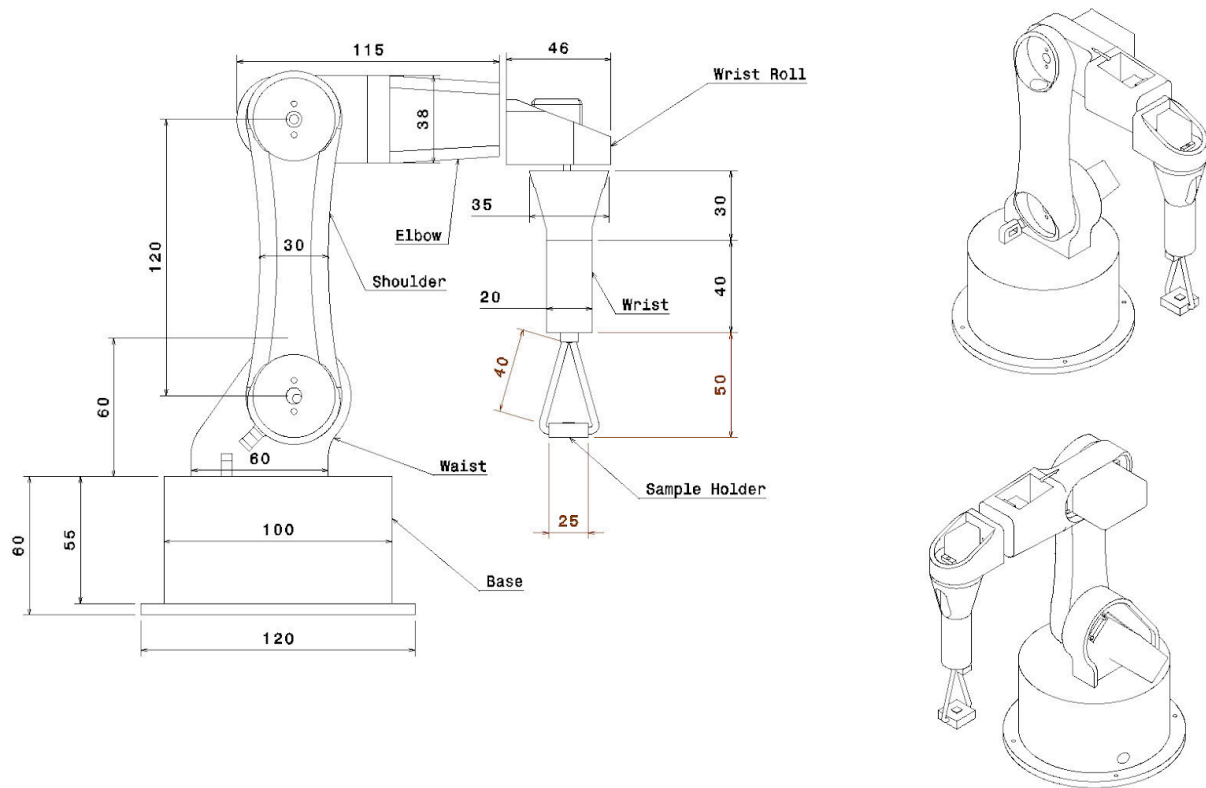


**Figure 10:** 2D Side View Of Robotic Arm

Servo motors are required to move the joints of the robotic arm and in our project, we have incorporated two types of servo motors to construct the robotic arm which are programmed to rotate the arm in the desired direction.

#### ❑ MG-996R SERVO MOTOR

The MG996R is a metal gear servo motor with a maximum stall torque of 11 kg/cm. Like other RC servos the motor rotates from 0 to 180 degree based on the duty cycle of the PWM wave supplied to its signal pin. As we know there are three wires coming out of this motor. The description of the same is given on top of this page. To make this motor rotate, we have to power the motor with +5V using the Red and Brown wire and send PWM signals to the Orange colour wire. Hence we need something that could generate PWM signals to make this motor work, we are using an Arduino Microcontroller.



**Figure 11:** Image of MG-996R Servo Motor

### Wire Configuration

Wire Number	Wire Color	Description
1	Brown	Ground wire connected to the ground of system
2	Red	Powers the motor typically +5V is used
3	Orange	PWM signal is given in through this wire to drive the motor

**Table 1:** Wire configuration of MG-996R servo motor

### MG996R Servo Motor Features

- Operating Voltage is +5V typically
- Current: 2.5A (6V)
- Stall Torque: 9.4 kg/cm (at 4.8V)
- Maximum Stall Torque: 11 kg/cm (6V)
- Operating speed is 0.17 s/60°
- Gear Type: Metal
- Rotation : 0°-180°
- Weight of motor : 55gm

### ❑ MG-90S SERVO MOTOR

MG-90S is a micro servo motor with metal gear. This small and lightweight servo comes with

high output power, thus ideal for RC Airplane, Quadcopter or Robotic Arms.



**Figure 12:** Image of MG90S servo motor

### Wire Configuration

Wire Number	Wire Color	Description
1	Brown	Ground wire connected to the ground of system
2	Red	Powers the motor typically +5V is used
3	Orange	PWM signal is given in through this wire to drive the motor

**Table 2:** Wire configuration of MG90S servo motor

### MG90S Servo Motor Features:

- Operating Voltage: 4.8V to 6V (Typically 5V)
- Stall Torque: 1.8 kg/cm (4.8V)
- Max Stall Torque: 2.2 kg/cm (6V)
- Operating speed is 0.1s/60° (4.8V)
- Gear Type: Metal
- Rotation : 0°-180°
- Weight of motor : 13.4gm

### **2.3.2. Assembling of Robotic Arm**

**Step 1-**Assembling the MG servo to the Base of robotic arm.

Initially the MG-996r Servo motor is fixed to the base of the robotic arm.

**Step 2-** Assembling the waist to the base of robotic arm:Screw the waist using two screws to the servo roll of the base of robotic arm and also fix the MG-996r servo to the waist using two screws.

**Step 3-** Assembly of the shoulder to the waist:Fix the roll of the servo to the Shoulder one end using two screws and then fix the servo and shoulder by using the screw.

**Step 4-** Assemble the servomotor to the elbow: Screw the MG-996r servo motor to the Elbow.

**Step 5-** Assembly of the Elbow to the shoulder :Fix the MG- 996r servo to the Elbow and then fix the Elbow and shoulder to together using the roll provided with the servomotor.

**Step 6-** Assembly of servo motor to elbow to attach wrist roll: Attach the MG-90 Servo motor from inside of the gap given in the servo motor using the screws provided with the servomotor.

**Step 7-** Assemble the wrist roll to the Elbow: Attach the wrist roll to the elbow mg-90 servo motor by using the screw.

**Step 8-** Assemble servomotor to the wrist roll: Attach the MG-90 servo motor to the wrist roll using two screws.

**Step 9-** Attach the wrist and the sample holder to the wrist roll servo motor using screws.

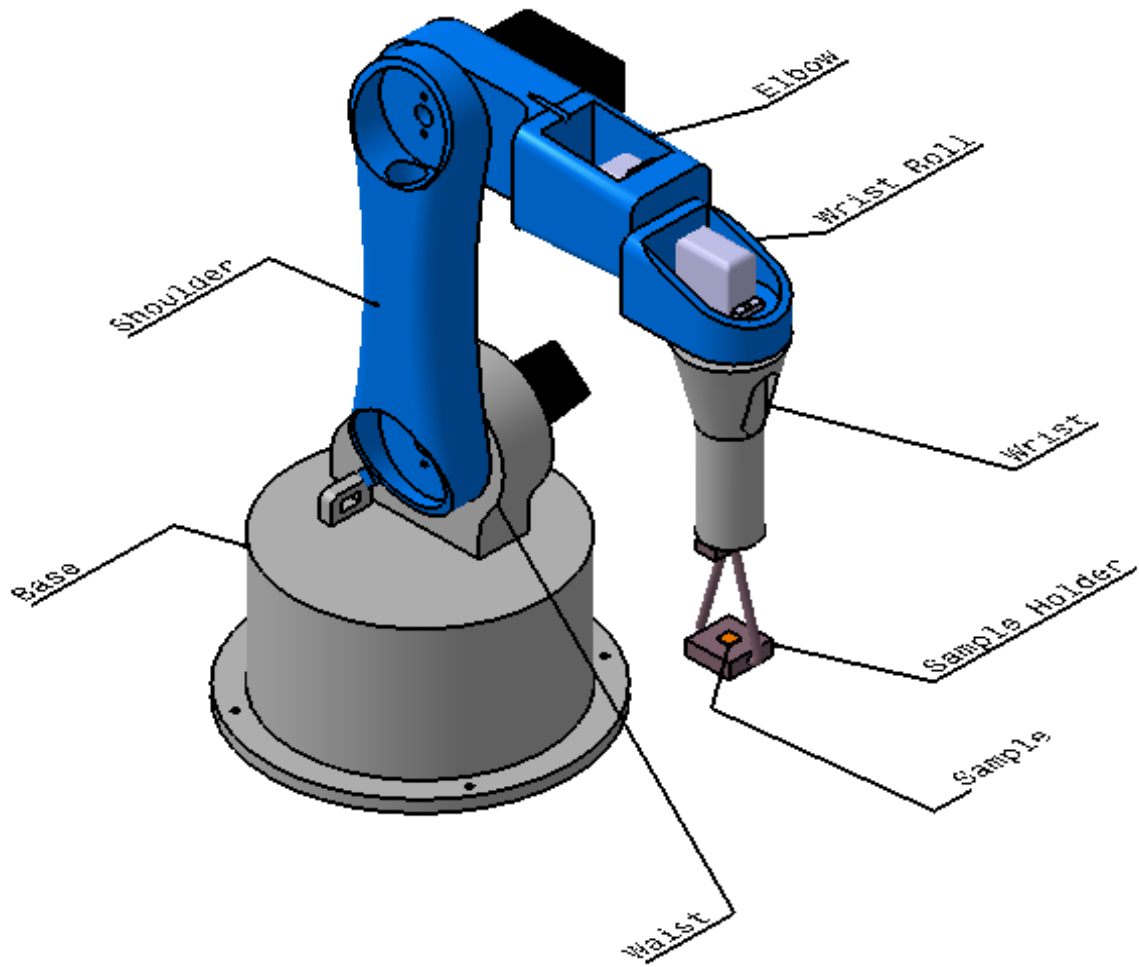


**Figure 13:** 3D Side View Of Robotic Arm

#### **2.4. AUTOMATION OF ROBOTIC ARM**

The automation of the Robotic Arm is done with the help of Arduino UNO Microcontroller. Arduino UNO is an open-source microcontroller board based on the Microchip ATmega328P microcontroller and developed by Arduino.cc. The board is equipped with sets of digital and analog input/output (I/O) pins that may be interfaced to various expansion boards (shields) and other circuits. The board has 14 Digital pins, 6 Analog pins, and programmable with the Arduino IDE (Integrated Development Environment) via a type B USB cable. It can be powered by a USB cable or by an external 9 volt battery, though it accepts voltages between 7 and 20 volts. The ATmega328 on the Arduino Uno comes pre-programmed with a bootloader that allows

uploading new code to it without the use of an external hardware programmer. It communicates using the original STK500 protocol. The Uno also differs from all preceding boards in that it does not use the FTDI USB-to-serial driver chip. Instead, it uses the Atmega16U2 (Atmega8U2 up to version R2) programmed as a USB-to-serial converter.

The first phase is the software development which is done using Arduino Integrated Development Environment(IDE) Programming software. For software programming, an assembly language was used to construct the command to get the desired results. Assembly language can be used to specify the exact instructions and one can control the time and space(memory) used for each step of the program. Three servo motors(SERVO1, SERVO 2 and SERVO 3) of the robotic arm are interfaced with the Arduino board which are programmed to achieve the rotation of the robotic arm as well as the sample holder in desired direction to take the measurements. The 3 servo motors used at each axis is connected to the arduino through the input pins. The rotation of the servo motor is controlled by providing it with a pulse width modulated signal.

Eg: (pos=0; pos<180; pos+=10)

myservo.write(pos); \\pos provides the position it needs to move

Here the servo motor moves from left to right, ranging from  $0^\circ$  to  $180^\circ$ . In the same manner each servo motor can be programmed to rotate at a certain angle to obtain a particular position of the sample between the magnets. Next step is to upload the programming code into ATmega328 and all the variables to be used is written down on it. The programming interprets and sends to PIC. The input and output is declared. After this process has complete, the program will analyze and run it on Arduino Uno to identify and detect if there is any failure in programming before loading to ATmega328. Next step is to upload it via universal serial bus (USB). The USB-to-serial adapter chip or cable is implemented through USB interface. After sending the command via USB to ATmega328, the programming will be analyzed again to the electronic component to work.

The below Fig. 14 represents the interfacing connection diagram of the Arduino and servo motors. Servomotor\_1 is connected to pin 6 of the arduino, Servomotor\_2 is connected to pin 7 of the arduino and Servomotor\_3 is connected to pin 9 of the arduino.

Vcc pin of the Arduino is connected to all the Vcc pins of the servomotor's and similarly the ground pin of Arduino is connected to ground pins of the servomotors.

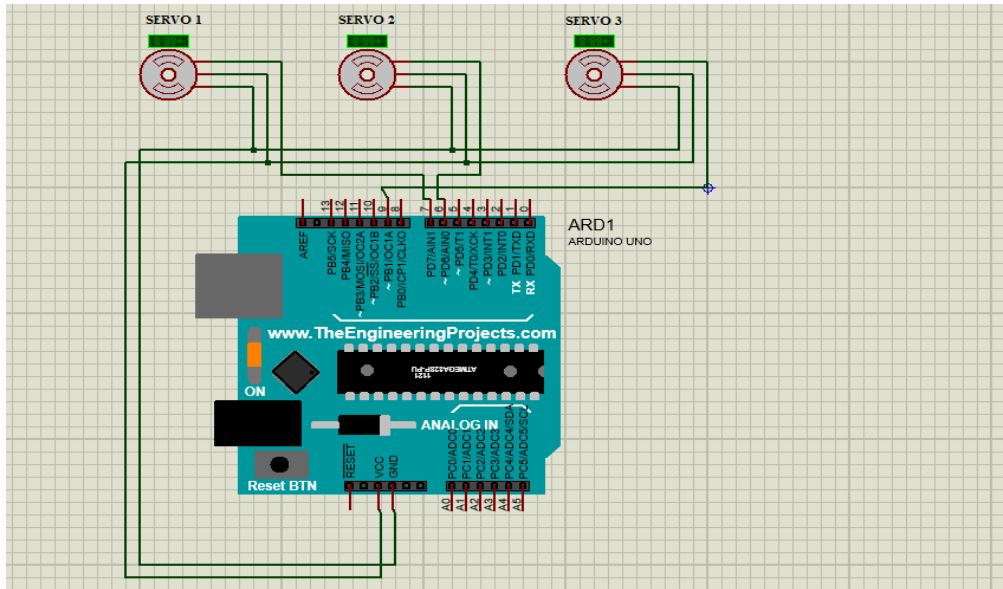


**Figure 14:** Interface of servo motors with Arduino

The flowcharts given below represent the two programs used to control the robotic arm. Fig. 15a represents the 180 degree rotation of the servo motor needed for the rotation of sample which is placed on the sample holder. Servomotor\_1 is set to 95 degrees and servomotor\_2 is set to 28 degrees. We then start a loop in which a variable ‘pos’ is called which counts the turns of rotation of the servomotor\_3. The servomotor\_3 is then incremented with every 10 degrees. This will rotate the sample every 10 degree which will help us to take in the set of readings in the presence of the magnetic field. Fig. 15b represents the movement of the robotic arm out of the magnetic field area, so as to replace the sample. When the program is initiated the servomotor\_1 will be set to 125 degrees and servomotor\_2 will be set to 10 degrees. This will then help us to take the sample out of the sample holder and replace it with a new sample.

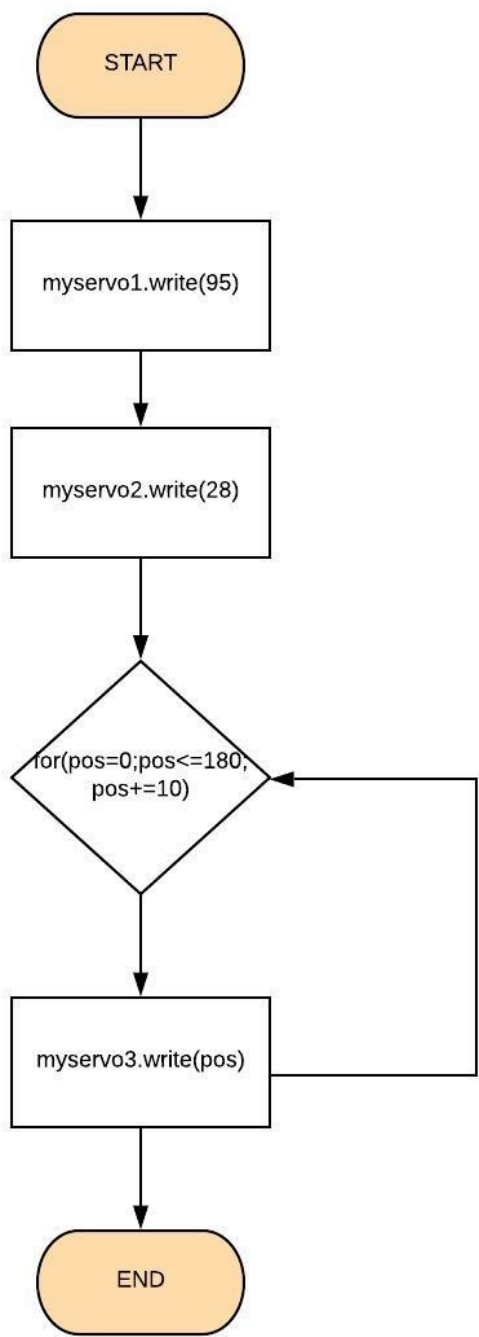
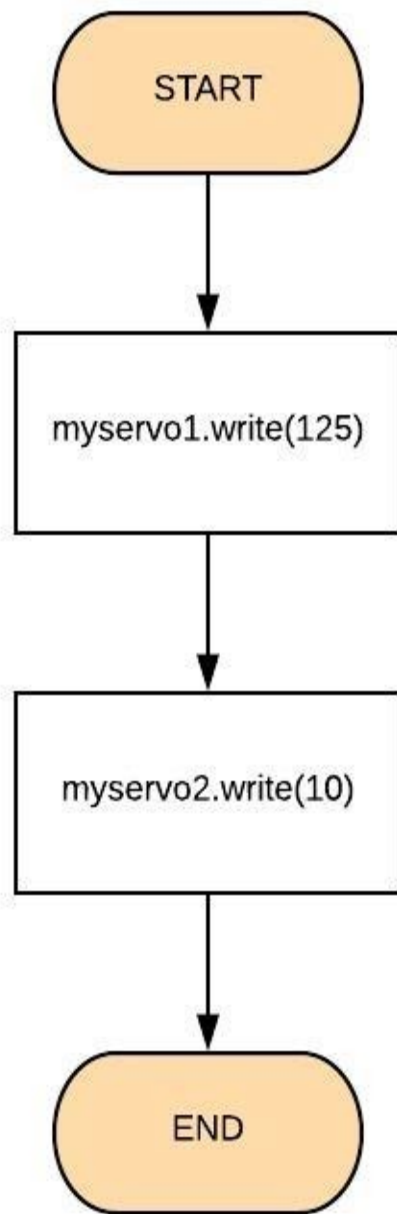


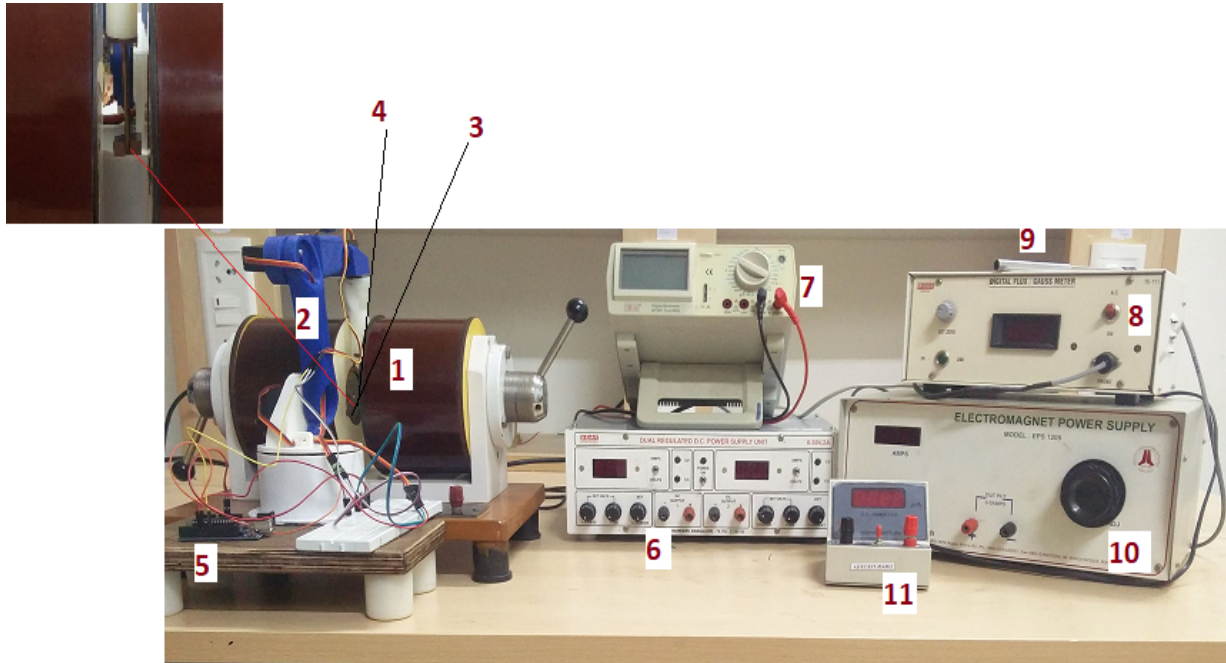
**Figure 15 a:** Flowchart for the rotation of Robotic Arm



**15b:** Flowchart for Up and Down movement of Robotic Arm

## 2.5. ASSEMBLY OF TRANSPORT MEASUREMENT SYSTEM

The final assembly of the electromagnetic transport measurement system is shown in the below figure 15.



- 1.Electromagnet; 2.Robotic Arm; 3.Sample Holder; 4.Sample; 5.Arduino UNO Board;
- 6.DUAL REGULATED DC POWER SUPPLY; 7.DC MULTIMETER; 8.GAUSSMETER;
- 9.GAUSS PROBE; 10.ELECTROMAGNETIC POWER SUPPLY; 11.DC AMMETER

**Figure 16:** Final Assembly of transport measurement system

The electromagnet is setup and with the help of gauss meter and electromagnetic power supply, the electromagnet is calibrated. The robotic arm is designed and fabricated according to the specifications with the help of servo motors. The sample holder is connected to the hand of the robotic arm upon which the sample is placed and kept exactly in the center between the two poles of the electromagnet. The servo motors of the robotic arm are programmed using Arduino uno to move between 0 degree to 180 degree. The sample is fabricated and connections are done using two probe method. In this method two thin 50 $\mu$ m copper wires are connected on the 5mm $\times$ 5mm sample with help of silver paste and thinner. One of the copper wire is connected to voltage supply and another connected to ammeter and then placed on the sample holder made of copper. The sample holder that holds the sample is rotated in the desired direction with help of

robotic arm that is powered up by the Arduino Uno Microcontroller. Different voltage levels are applied and current values are noted down for every 10 degree of sample rotation and hence both isotropic and anisotropic measurements are performed. An I-V characteristics graph is plotted and magnetoresistance is measured.

### **2.5.1. Unique Features of Transport Measurement System**

The availability of spin transport measurement system in India is very limited. The existing systems can measure only in-plane and out-of-plane measurements. Some of them are automated and bulky. The transport measurement system that we have fabricated is an automated and compact system from lab point of view. The unique features of the system is that it can perform both isotropic and anisotropic measurements. In isotropic measurement, the sample can be rotated at any degree variation ranging from 0°-180°.

## CHAPTER 3

### DEMONSTRATION OF DEVELOPED TRANSPORT MEASUREMENT SYSTEM

#### **3.1. FABRICATION OF SAMPLE**

The sample we are fabricating for our project is Fe<sub>3</sub>O<sub>4</sub>/Si. The substrate we are using is silicon wafer over which a ferrimagnetic material Fe<sub>3</sub>O<sub>4</sub> is deposited. The technique used for the deposition is PLD (Pulsed laser Deposition) Technique. The reason we are using silicon as substrate is because it is already an existing technology and could be easier to manufacture. Different crystal substrates such as Ge (001), Ge(111), GaAs and MgO have been used to prepare thin films. This is a limitation because most crystal substrates are expensive and unsuitable for large-scale production. On the other hand, Si is considered to be a superior semiconductor owing to its long spin lifetime and overwhelming dominance .So it is necessary to determine the structural and ferromagnetic properties of films on Si substrate.

#### **Specification**

- Dimensions: (5mmx5mm) or (8mmx8mm)
- Technique:Pulsed laser deposition (PLD)
- Thickness of the film:30 nm
- Substrate: Semiconductor Material
- Deposited layer: Ferrimagnetic material
- Heterojunction: Fe<sub>3</sub>O<sub>4</sub>/SiO<sub>2</sub>/ Si

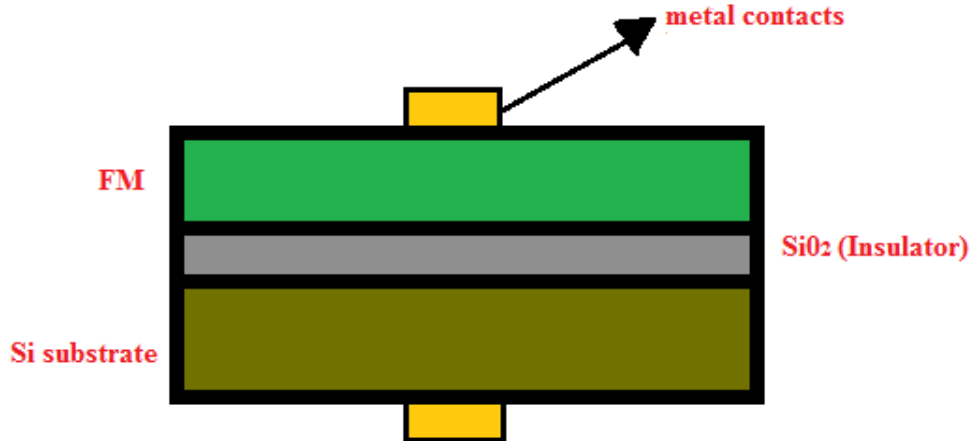


**Figure 17:** Heterostructure sample

### 3.2. PULSED LASER DEPOSITION

**Pulsed LASER Deposition** is thin film deposition technique in which highly energetic pulsed LASER beam is focused on the target material in presence of vacuum or controlled background gas environment. This causes the vaporization of target material in form of plasma plume which is deposited as thin film on the substrate. Stoichiometry and roughness of the film can be controlled by manipulating LASER parameters, gas pressure inside the chamber and substrate temperature. This material is vaporized from the target (in a plasma plume) which deposits it as a thin film on a substrate (such as a silicon wafer facing the target). When the laser pulse is absorbed by the target, energy is first converted to electronic excitation and then into thermal, chemical and mechanical energy resulting in evaporation of the target which is deposited on the substrate. The ejected species expand into the surrounding vacuum in the form of a plume containing many energetic species including atoms, molecules, electrons, ions before depositing on the typically hot substrate. The advantages of PLD are:

- Conceptually simple: a laser beam vaporizes a target surface, producing a film with the same composition as the target.
- Cost-effective: one laser can serve many vacuum systems.
- Versatile: many materials can be deposited in a wide variety of gases over a broad range of

gas pressures.

- Fast: high quality samples can be grown reliably in 10 or 15 minutes.

The unit is comprised of two parts: LASER and deposition chamber;

#### LASER specifications:

- Wavelength : 248 nm
- Pulse width : 25 nsec
- Energy : 250 – 750 mJ
- Repetition rate : 1 – 50 Hz

#### Chamber specifications:

- Chamber consists of six target holders and one substrate holder for multilayer deposition.
- Base pressure can be reached up to  $\sim 10^{-7}$ mbar with the help of rotary and turbo molecular pump.
- Presently highly pure oxygen is used for deposition and the pressure is controlled using mass flow controller with precession of 0.1 mbar.
- Maximum substrate can be reached up to 750° C.
- Completely automated deposition process.

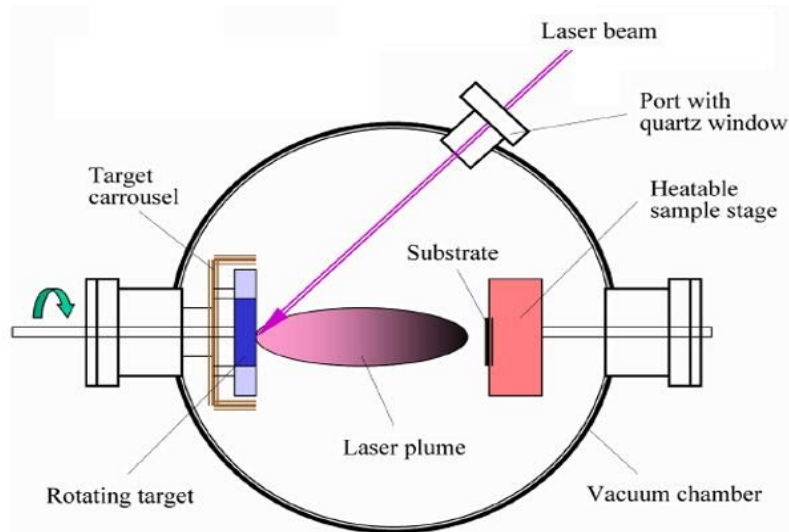


**Figure 18:** PLD Chamber

### **3.3 EXPERIMENTAL DETAILS**

Fe<sub>3</sub>O<sub>4</sub>/p-Si heterostructures were fabricated by pulsed laser deposition (PLD) technique. The substrate was pre-cleaned by a standard piranha chemical method. Initially, the substrates were dipped in acetone under ultrasonic agitation for 10–15 minutes and then rinsed in de-ionized (DI) water five times to remove oil contamination as well as dust particles attached to the semiconductor substrates. Further, the substrates were cleaned in methanol, trichloro ethanol and finally again in acetone under ultrasonication before rinsing in DI water. Next the Si (1 11) substrates were cleaned with 1:1 H<sub>2</sub>O<sub>2</sub>:H<sub>2</sub>SO<sub>4</sub> solution for 15 min and finally etched in HF(Hydrofluoric) solution before loading into the PLD chamber. A focused laser beam from a KrF laser source with a wavelength of 248 nm, repetition rate of 10 Hz and an energy density of 320 mJ at the solid Fe<sub>3</sub>O<sub>4</sub> target (solid targets were prepared from synthesized nanoparticles of the Fe<sub>3</sub>O<sub>4</sub> using the sol-gel method) for the laser ablation was used. The Fe<sub>3</sub>O<sub>4</sub> thin films were fabricated on a p-Si substrate under a base pressure of  $2 \times 10^{-5}$  mbar without any ambient gas and the substrate temperature was kept at 360 °C during the deposition of the Fe<sub>3</sub>O<sub>4</sub> films. The structures of the thin films and the sharpness of the interfaces were studied using a high resolution x-ray diffractometer, planar high-resolution transmission electron microscopy (HR-TEM) and cross-sectional high-resolution transmission electron microscopy (HR-XTEM) measurements.

### **3.4. FILM DEPOSITION**

The pivotal motif of spin transport electronics is to control and active manipulation of electron spin degree of freedom in semiconductors. The tunneling of spin polarized electrons is the most promising way to achieve spin injection from a ferromagnetic material (FM) into semiconductors (SC), through an insulating tunnel barrier in FM/SC heterostructure. Several experimental reports on injection of spin polarized current into the SC from ferromagnetic metals (FMM)or dilute magnetic semiconductors (DMS) are found in literature. The image below of the Fe<sub>3</sub>O<sub>4</sub>/Si heterostructure shows that the interface of the Fe<sub>3</sub>O<sub>4</sub>/Si heterostructure contains a very thin uniform native oxide (SiO<sub>2</sub>) layer with a thickness of about 2 nm. This native oxide layer may serve as a tunnel barrier for the spin-polarized transport in Fe<sub>3</sub>O<sub>4</sub>/SiO<sub>2</sub>/

Si heterostructures. The thickness of the film is about 30 nm.

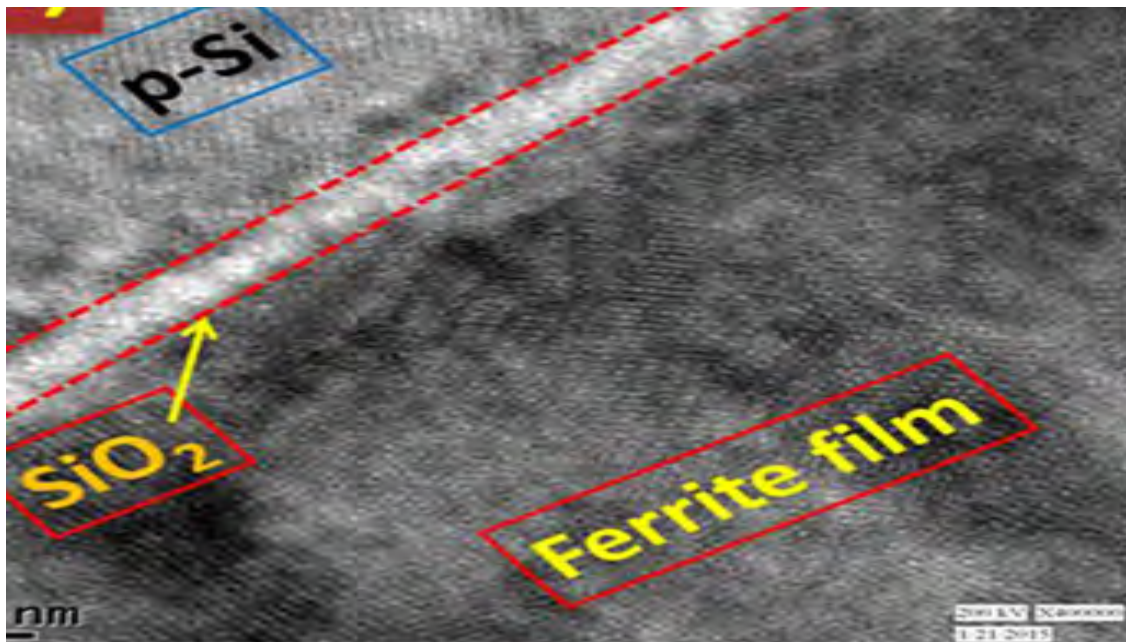


**Figure 19:** Image of Film deposition

### 3.5. FERRIMAGNETIC MATERIALS

Ferrimagnetism is a special case of antiferromagnetism where the magnetic moments on the two sublattices while still pointing in opposite directions have different magnitudes. The ferrimagnetic materials behave on macroscopic scale very much like ferromagnetic materials. They have a spontaneous magnetization below the Curie temperature and are organized into domains. They also exhibit hysteresis and saturation in their magnetization curves. Ferrimagnetic materials are the salts of the transition metals, particularly which crystallize in the spinel structure and contain in some measure one of the known ferromagnetic elements viz. cobalt, iron, nickel etc. They are called ferrites. The classical formula of the ferrite is  $AB_2O_4$ , where A represents a variety of divalent metal cations ( $Fe^{2+}$ ,  $Co^{2+}$ ,  $Ni^{2+}$ ,  $Zn^{2+}$ ,  $Cu^{2+}$ ,  $Mn^{2+}$  and so on), B represents trivalent metal ions (mostly  $Fe^{3+}$ ), and O the oxygen anion. The general formula of ferrite may be expressed as  $MO\cdot Fe_2O_4$  (or sometimes,  $M^{2+}Fe_2^{3+}O_4^{2-}$ ) with M the divalent metal ions. The most familiar example of ferrimagnetic material is magnetite whose chemical formula is written as  $Fe_3O_4$ .

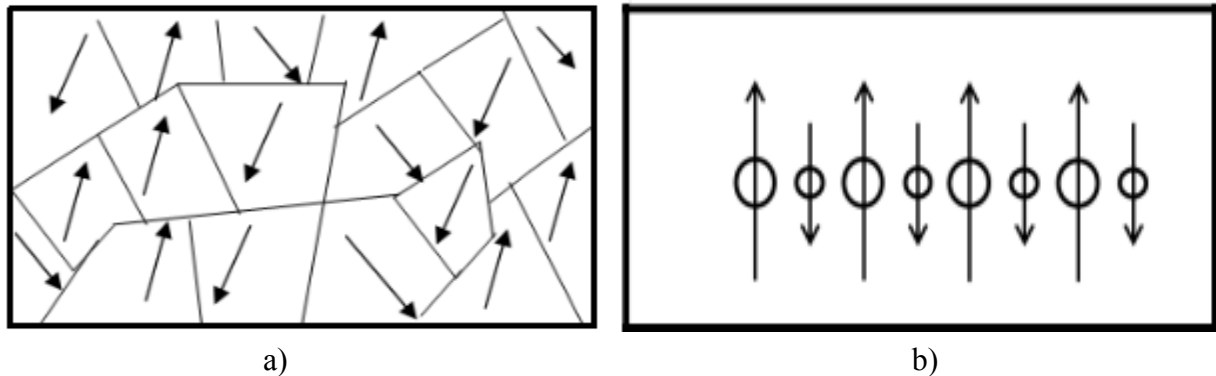


**Figure 20:** Orientation of ferrimagnetic material: a) Random domain orientation b) After magnetization

### Properties of Ferrimagnetic Materials

- If a ferrimagnetic material is placed under an external magnetic field of strength  $H$ , the magnetization  $M$  of the material can be altered producing a magnetization .
- Magnetic properties of Ferrimagnetic materials strongly depend on the particle size .
- The ferrimagnetism mechanism is not present in liquids and gases.
- The Curie temperature of a ferrimagnetic material is  $\sim 851$  K
- The intensity of magnetization ( $M$ ), magnetic susceptibility ( $\chi_m$ ), relative permeability ( $\mu_r$ ), and magnetic flux density ( $B$ ) of this material will be always prominent and positive.

$$\begin{aligned}\chi_m &= \frac{M}{H} \\ \mu_r &= 1 + \chi_m \\ B &= \mu_0(H + M)\end{aligned}$$

$\mu_0 \rightarrow$  Magnetic permittivity of free space.

$H \rightarrow$  Applied peripheral magnetic field strength.

<b>Mineral</b>	<b>T<sub>N</sub>(K)</b>	<b>M<sub>s</sub>(Am<sup>2</sup>/kg) at 300K</b>
Pyrrhotite(Fe <sub>7</sub> S <sub>8</sub> )	593	20
Jacobsite(MnFe <sub>3</sub> O <sub>4</sub> )	673	77
Daubreeelite	~170	~30(at 70K)
Fe <sub>2</sub> O <sub>3</sub>	~510	~15
Greigite(Fe <sub>3</sub> S <sub>4</sub> )	>593	59
Fe <sub>3</sub> O <sub>4</sub>	~851	~91

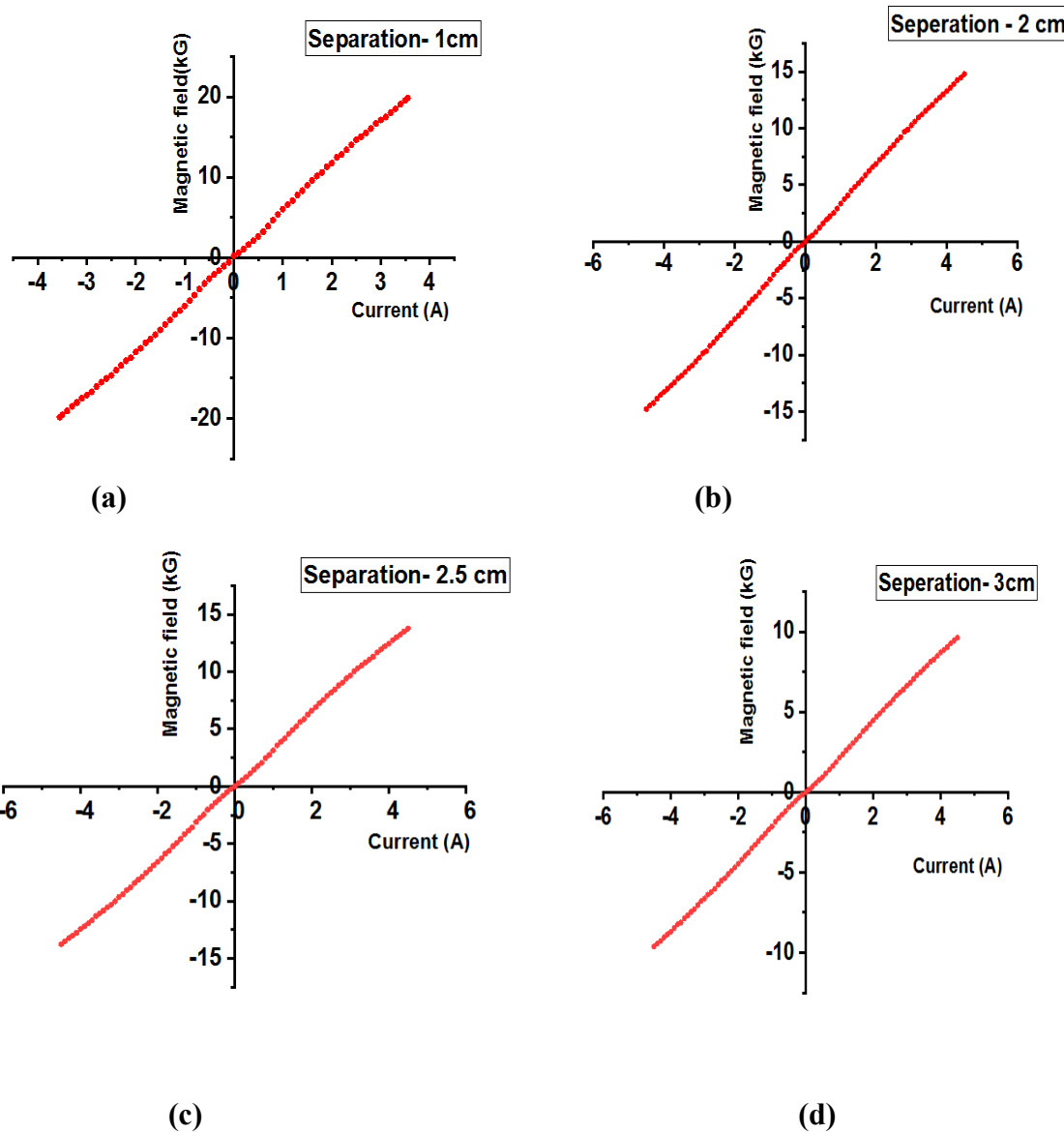
**Table 2:** Comparison of Ferrimagnetic materials

From above materials, Fe<sub>3</sub>O<sub>4</sub> is used for spin injection because it has more spins and shows higher magnetization property compared to others at room temperature.

### **3.6. CALIBRATION OF INSTRUMENTS**

#### **3.6.1. Electromagnet**

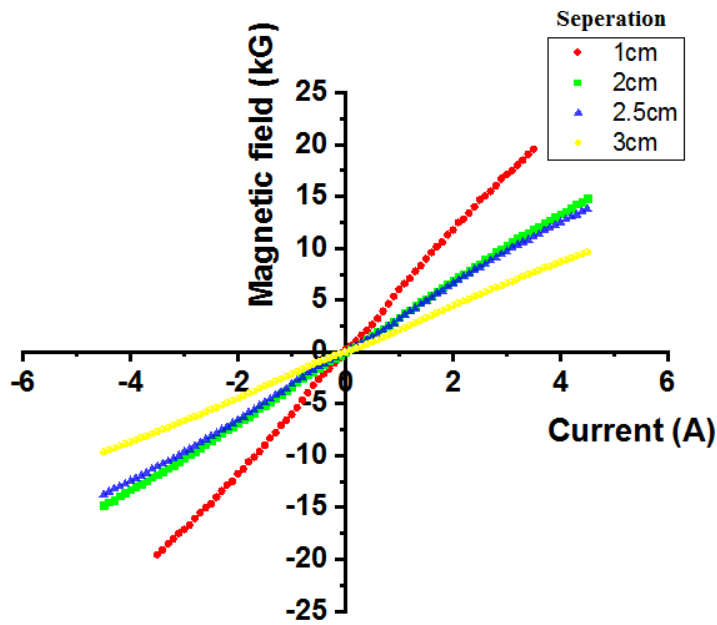
The strength of the magnetic field of the electromagnet is determined using a gauss meter, gauss probe and a current supply source varying from 0 A-5 A. The gauss probe which is a hall sensor is placed exactly between the two poles of the electromagnet and the separation between the poles is varied from 1cm to 3cm. A varying current is supplied from the electromagnetic power supply to the electromagnet from a range of 0 A-5 A in steps of 0.1, whose corresponding magnetic field strength is recorded in the gaussmeter. The range of the gauss meter is 0kG-20kG.



**Figure 21:** Calibration of electromagnet:a) poles are separated by 1cm; b) poles are separated by 2cm; c)poles are separated by 2.5cm; d) poles are separated by 3cm;

From the above experiment, we came to a conclusion that strength of magnetic field is inversely proportional to the distance of the poles i.e if the distance between the poles is shorter, the magnetic field is higher and vice-versa. The above images shows a linear graph of magnetic field vs current for different separation of poles. Fig. 21a shows a graph whose separation between the two poles is 1 cm and at current equal to 4 A, the corresponding magnetic field strength is 20 kG(maximum range) making the electromagnet highly unstable. In fig. 21b,

where separation between the poles is 2 cm, at current 5 A the maximum magnetic field strength observed is 15 kG. In fig. 21c with separation between the poles is 2.5 cm, at current 5 A the maximum magnetic field strength observed is 13 kG and in fig. 20d with separation between the poles 3 cm, the maximum magnetic field strength observed at 5 A is 10 kG. We have considered 2.5 cm and 3 cm pole separation for our instrument keeping in mind the stability of the electromagnet, space constraint between the poles.

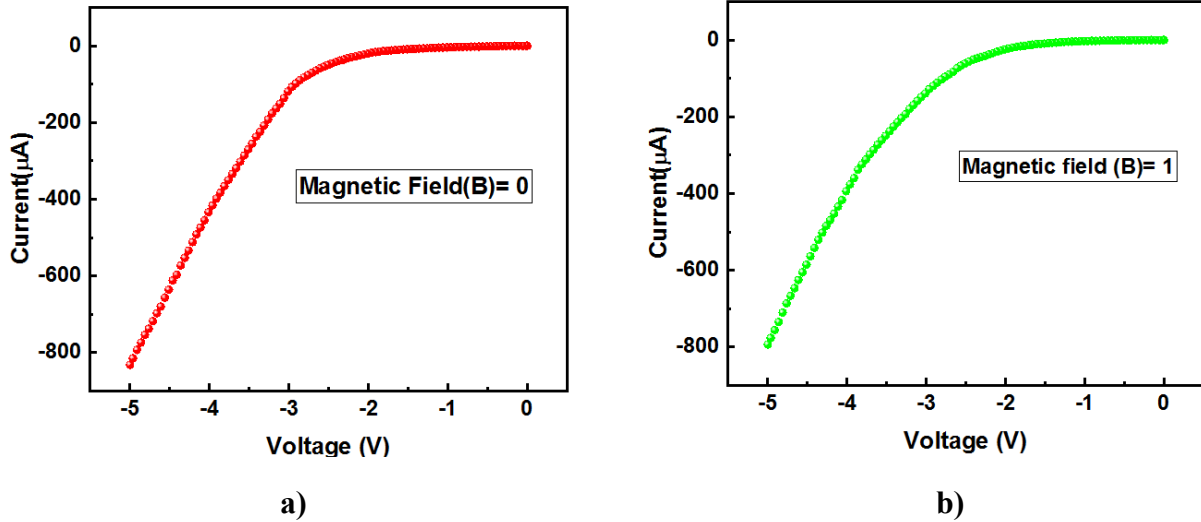


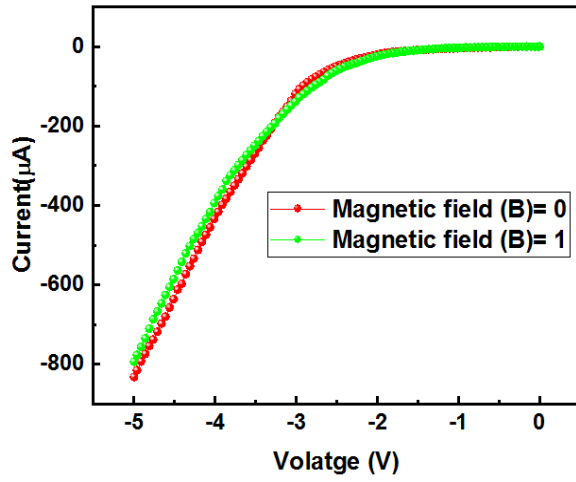
**Figure 22:** Comparison of magnetic field vs current at different separations of the poles.

Fig. 22 gives a more detailed comparison of magnetic field vs current at different separations of the poles. Red line on the graph indicates magnetic field strength at 1 cm separation, Green line indicates magnetic field strength at 2 cm, blue line indicates magnetic field strength at 2.5 cm and yellow line indicates magnetic field strength at 3 cm. We observe that the magnetic field strength produced by the electromagnet at a distance of 1 cm between the poles is much higher compared to 3 cm . For an optimum scenario, 3 cm pole distance is chosen such that the stability and performance of the electromagnet will not be affected even though the field produced is comparatively lesser, and thereby providing higher mobility of the sample holder placed between the two poles.

### 3.7. RESULTS AND DISCUSSIONS

The preliminary step prior to transport measurements is conducting hall measurement of the sample which will describe the type of carrier and the carrier concentration of the film and substrate. The RT Hall measurements show the hole (p-type) carrier concentration of  $1.04 \times 10^{15} \text{ cm}^{-3}$  for the p-Si substrate and  $2.44 \times 10^{19} \text{ cm}^{-3}$  for Fe<sub>3</sub>O<sub>4</sub> thin film. The p-type semiconducting behavior of the Fe<sub>3</sub>O<sub>4</sub> may be due to the vacancies of the metal cation (Fe<sup>3+</sup>) in octahedral sites. Because the parent Fe<sub>3</sub>O<sub>4</sub> film shows the hole carrier concentration of  $2.44 \times 10^{19} \text{ cm}^{-3}$ , one can consider this film as a highly doped p-type semiconducting ferromagnet (p++-Fe<sub>3</sub>O<sub>4</sub>) compared to p-Si, and can anticipate that the Fermi level (E<sub>f1</sub>) of the Fe<sub>3</sub>O<sub>4</sub> film is close to the valence band. Magnetite or Fe<sub>3</sub>O<sub>4</sub> is ferrimagnetic at room temperature and has high Curie temperature T<sub>c</sub> = 851 K [51]. Beyond T<sub>c</sub>, Fe<sub>3</sub>O<sub>4</sub> becomes disordered and loses its magnetization due to thermal energy leading to a paramagnetic state.





c)

**Figure 23:** I-V characteristics of  $\text{Fe}_3\text{O}_4/\text{SiO}_2/\text{p-Si}$  heterostructure: a) with the magnetic field of 0 T at 300 K; b) with the magnetic field of 1 T at 300 K; c) at 300 K for the ON (1 T, red line) and OFF (0 T, green line) condition of magnetic field

For the transport measurement, the sample is biased i.e, connecting a voltage potential across it. +ve terminal of the supply is connected to the p-type substrate (Si substrate) and -ve terminal is connected to magnetite film ( $\text{Fe}_3\text{O}_4$ ) where reverse bias characteristics are observed. Fig. 23(a) represents a graph of current vs voltage in the absence of magnetic field. Notably, the I-V characteristics of heterostructure in Fig. 23(a) exhibit a perfect backward rectifying property. Fig. 23(b) represents a graph of current vs voltage in the presence of magnetic field. The magnetic field of 1 T was chosen in our transport measurements to keep the  $\text{Fe}_3\text{O}_4$  film in saturation magnetization condition. Fig. 23(c) shows I-V characteristics of  $\text{Fe}_3\text{O}_4/\text{SiO}_2/\text{p-Si}$  heterostructure when the magnetic field is in OFF (0 T, Red line) and ON (1 T, Green line) conditions at room temperature. The magnetic field was applied perpendicular to the current. It is very interesting to note that the current under magnetic field as a function of reverse bias is not monotonously decreasing or increasing with respect to the current under zero field, rather the crossover between the two current curves around 3.2 V is observed. At lower voltage region also, there is a crossover around 1.4 V.

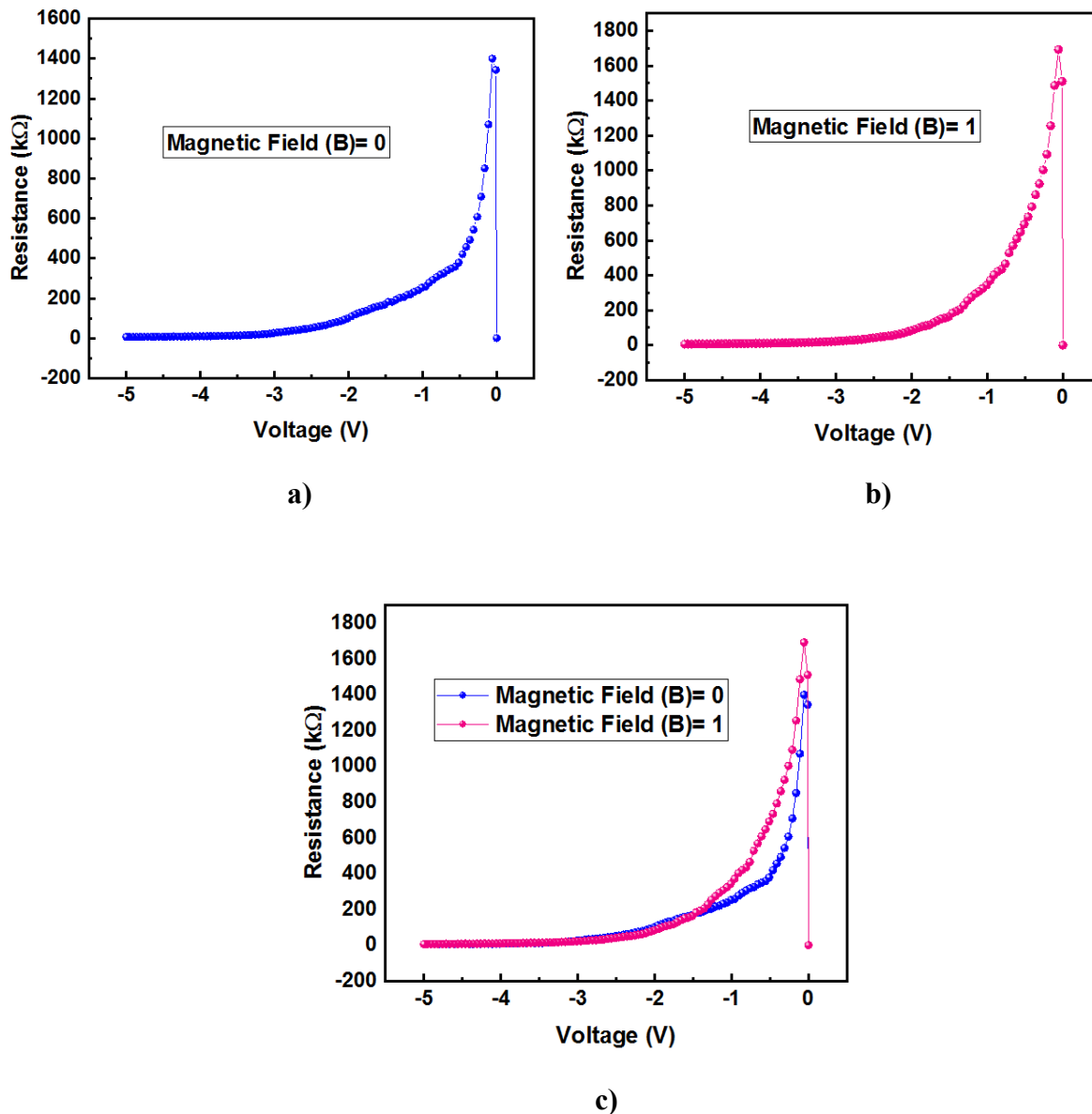


**Figure 24:** Resistance vs voltage characteristics of Fe<sub>3</sub>O<sub>4</sub>/SiO<sub>2</sub>/p-Si heterostructure: a)with the magnetic field of 0 T; b)with the magnetic field of 1 T; c) at 300 K for the ON (1 T, pink line) and OFF (0 T, blue line) condition of magnetic field

The above graph represents a resistance vs voltage characteristics of the heterostructure sample. Fig.24a represents a graph of resistance vs voltage in the absence of magnetic field. We observe higher resistance at lower negative voltage as the current produced by the sample at this voltage is very low. As negative voltage increases we observe gradual decrease in the resistance. At lower voltage region, there is a crossover around 1.4 V after which there is similar

characteristics are observed in both ON and OFF conditions of the magnetic field. The recorded values of resistance in both ON and OFF conditions of magnetic field are used to calculate the magnetoresistance of the sample. The MR is termed as a JMR which is the total resistance of the given heterostructure, including the junction/interface effect, and defined as,

$$MR \% = \frac{\Delta R}{R} \times 100\% = \frac{(R(B \neq 0)) - (R(B=0))}{(R(B=0))} \times 100\%$$

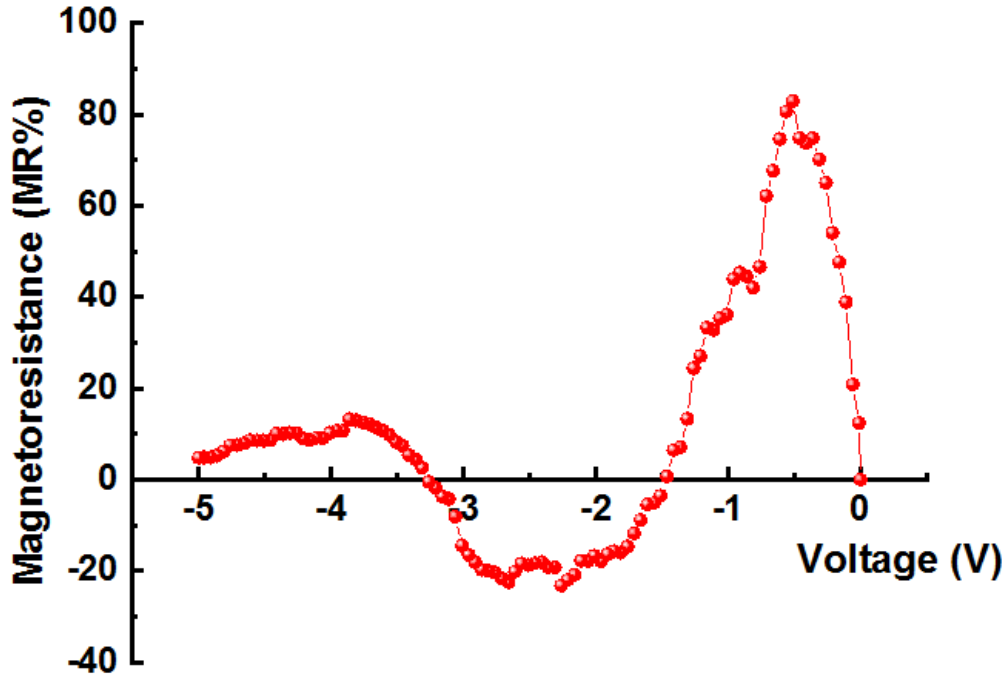


**Figure 25:** Bias voltage dependence of junction magnetoresistance (JMR) of Fe<sub>3</sub>O<sub>4</sub>/SiO<sub>2</sub>/p-Si heterostructure on application of B=1 T at T= 300 K (RT)

Fig. 25 shows the bias voltage dependence of MR of Fe<sub>3</sub>O<sub>4</sub>/SiO<sub>2</sub>/p-Si heterostructure on application of 1 T magnetic field at RT. The MR of the Fe<sub>3</sub>O<sub>4</sub>/SiO<sub>2</sub>/p-Si heterostructure referred includes the resistance of ferromagnetic Fe<sub>3</sub>O<sub>4</sub> film, native oxide (SiO<sub>2</sub>) layer, and semiconducting substrate (p-Si), in addition to the junction/interface effect.

At room temperature, we observed large positive and negative JMR of 83% and 23% at 0.5 V and 2.2 V bias voltage, respectively. The response of the device against the magnetic field at RT is explored by measuring the reverse bias current as a function of the magnetic field at selected negative voltage and calculated the corresponding MR values shown in inset of Fig. 25. The positive JMR of the device at 1 V, 5 V and negative MR at 2 V reflects the results of Fig. 25.

From the above results, the following interesting observations are made: (i) variation and sign change of JMR as a function of the bias voltage at room temperature and (ii) the JMR of the device is symmetric for both positive and negative magnetic field with respect to the zero field.

## CHAPTER 4

### CONCLUSION AND SCOPE OF FUTURE WORK

#### 4.1. CONCLUSION

In summary, a compact electromagnetic transport measurement system was fabricated to measure the magnetoresistance of the heterostructure sample which can help us analyze and determine which material is suitable for spintronic application. Initially, the electromagnet was calibrated to understand the maximum field strength produced by the adjustable air gap electromagnet for varying current supply. Then the Robotic Arm was designed to meet our specification where the robotic arm was fabricated using servo motors and programmed using Arduino UNO software. Three servo motors were interfaced with Arduino board and programmed for the rotation of sample holder to take both isotropic and anisotropic measurements. We have fabricated Fe<sub>3</sub>O<sub>4</sub>/SiO<sub>2</sub>/Si heterostructure using PLD process and studied the effect of electric field on the giant junction magnetoresistance property of the device. The device showed backward diode type behavior at room temperature and reverse bias dependent crossover like spin valve action with ON/OFF conditions of an external magnetic field. We have explained the origin of this backward rectifying feature and crossover of MR as a function of electric field by considering the electronic band structure of Fe<sub>3</sub>O<sub>4</sub>/SiO<sub>2</sub>/ p-Si heterojunction. The most important outcome of this study is the observation of enhanced MR and electrical dependence of MR other than the magnetic field dependence at room temperature, which may have a great importance in spintronics for device application. By fabricating such simple and compact system, it would be easier for everyone to work from laboratory point of view and explore more in the field of Spintronics. Spintronics is a field which depend on the spin of the electron, which has a great potential of spinning this global village into a unexpected digital atomic world which has a capability of manipulating at atomic level and this can even made further smaller. With the integration with new emerging technology called “nanotechnology”. This would make things smaller and cheaper and more affordable by a common man.

#### **4.2. FUTURE WORK**

The future work of this project is to perform the demonstration of the sample on the system we have fabricated and compare it with the standard values obtained. Secondly, to incorporate a bluetooth module which could help the user control the movement of the robotic arm through commands on smartphone via bluetooth. Thirdly, to measure the properties of the sample at different temperatures. Finally, to automate the entire system where real-time values can be obtained and graphs can be plotted simultaneously .

## REFERENCES

- [1] Xingxing Li and Jinlong. First principles design of spintronics materials Yang Article . April 2016 DOI: 10.1093/nsr/nww026.
- [2] Mukesh D Patil, Jitendra S Pingale,Umar I Masumdar . Overview of Spintronics, International Journal of Engineering Research & Technology, ISSN:2278-0181, Vol. 2, Issue-6, June-2013.
- [3] Wolf SA, Awschalom DD and Buhrman RA et al. Spintronics: a spin-based electronics vision for the future. *Science* 2001; 294: 1488–95
- [4] Giant magnetoresistance of (001)Fe/(001)Cr magnetic superlattices Baibich MN, Broto MM and Fert A et al.. *Phys Rev Lett* 1988; 61: 2472–5.
- [5] Silicon spintronics, Jansen R1, Nat Mater 2012 Apr 23;11(5):400-8. doi: 10.1038/nmat3293
- [6] H. Aireddy, S. Bhaumik, and A. K. Das. *Applied Physics Letters* 107, 232406 (2015); doi: 10.1063/1.4937391
- [7] H Aireddy and Amal K Das. 2016 *J. Phys. D: Appl. Phys.* 49 (2016) 415003(8pp)
- [8] M. Fonin, R. Pentacheva, Yu. S. Dedkov, M. Sperlich, D. V. Vyalikh, M. Scheffler, U. Rudiger, and G. Guntherodt, *Phys. Rev. B* 72, 104436 (2005).
- [9] D. Malinovska and M. Nikolaeva, *Vacuum* 69, 227–231 (2003).
- [10] M. Ahmetoglu, *Thin Solid Films* 516, 1227 (2008).
- [11] Purneshwari Varshney , Hemangi Agrawal. Spintronics Technology: A Review National Conference on Advances in Technology and Applied Sciences, at Jodhpur,

**March 2014**

- [12] S. A. Wolf ; A. Y. Chtchelkanova ; D. M. Treger. Spintronics—A retrospective and perspective
- [13] Abhishek Gautam. Spintronics - A New Hope for the Digital World International Journal of Scientific and Research Publications, August 2012, Volume 2, Issue 8, ISSN 2250-3153
- [14] I. Zutic', J. Fabian, and S. Das Sarma, Rev. Mod. Phys. 76, 323–410 (2004).
- [15] C. Chappert, A. Fert, and F. Nguyen van Dau, Nat. Mater. 6, 813–823 (2007).
- [16] S. P. Das, S. Sharma, R. S. Patel, M. P. Jong, and R. Jansen, Nature (London) 462, 491 (2009).
- [17] A. Fert and H. Jaffre's, Phys. Rev. B 64, 184420 (2001).
- [18] X. Lou, C. Adelmann, S. A. Crooker, E. S. Garlid, J. Zhang, K. S. M. Reddy, S. D. Flexner, C. J. Palmstrøm, and P. A. Crowell, Nat. Phys. 3, 197–202 (2007).
- [19] A. Sarker, R. Adhikari, and A. K. Das, Appl. Phys. Lett. 100, 262402 (2012).
- [20] M. N. Baibich, J. M. Broto, A. Fert, F. Nguyen Van Dau, F. Petroff, P. Eitenne, G. Creuzet, A. Friederich, and J. Chazelas, Phys. Rev. Lett. 61, 2472 (1988).
- [21] G. Binasch, P. Grunberg, F. Saurenbach, and W. Zinn, Phys. Rev. B 39, 4828 (1989).
- [22] S. Kohiki, T. Kinoshita, K. Nara, K. A. Hasegawa, and M. Mitome, ACS Appl. Mater. Interfaces 5, 11584–11589 (2013).
- [23] A. V. Ramos, M.-J. Guittet, J.-B. Moussy, R. Mattana, C. Deranlot, F. Petroff, and C. Gatel, Appl. Phys. Lett. 91, 122107 (2007).

- [24] J.-S. Kang, G. Kim, H. J. Lee, D. H. Kim, H. S. Kim, J. H. Shim, S. Lee, Hangil Lee, J.-Y. Kim, B. H. Kim, and B. I. Min, Phys. Rev. B 77, 035121 (2008).
- [25] K. Goto, T. Kanti, T. Kawai, and H. Tanaka, Nano Lett. 10, 2772–2776 (2010).
- [26] T. L. Qu, Y. G. Zhao, H. F. Tian, C. M. Xiong, and S. M. Guo, Appl. Phys. Lett. 90, 223514 (2007).
- [27] W. B. Mi, E. Y. Jiang, and H. L. Bai, J. Appl. Phys. 107, 103922 (2010).
- [28] J. M. D. Coey, A. E. Berkowitz, Ll. Balcells, and F. F. Putris, Phys. Rev. Lett. 80, 3815 (1998).
- [29] H. Y. Hwang, S. W. Cheong, N. P. Ong, and B. Batlogg, Phys. Rev. Lett. 77, 2041 (1996). 17K. I. Kobayashi, T. Kimura, H. Sawada, K. Terakura, and Y. Tokura, Nature (London) 395, 677–680 (1998).
- [30] Y. S. Dedkov, U. Rudiger, and G. Guntherodt, Phys. Rev. B 65, 064417 (2002).
- [31] D. J. Huang, C. F. Chang, H.-T. Jeng, G. Y. Guo, H.-J. Lin, W. B. Wu, H. C. Ku, A. Fujimori, Y. Takahashi, and C. T. Chen, Phys. Rev. Lett. 93, 077204 (2004).
- [32] S. F. Alvarado, W. Eib, F. Meier, D. T. Pierce, K. Sattler, H. C. Siegmann, and J. P. Remeika, Phys. Rev. Lett. 34, 319 (1975).
- [33] Chappert C, Fert A and Nguyen van Dau F 2007 Nat. Mater. 6 813
- [34] Fert A and Jaffrè H 2001 Phys. Rev. B 64 184420

- [35] Lou X, Adelmann C, Crooker S A, Garlid E S, Zhang J, Reddy K S M, Flexner S D, Palmstrøm C J and Crowell P A 2007 *Nat. Phys.* **3** 197
- [36] Jonker B T, Kioseoglou G, Hanbicki A T, Li C H and Thompson P E 2007 *Nat. Phys.* **3** 542
- [37] Das S P, Sharma S, Patel R S, Jong M P and Jansen R 2009 *Nature* **462** 491
- [38] Majumdar S, Das A K and Ray S K 2009 *Appl. Phys. Lett.* **94** 122505
- [39] Tian Y F, Deng J X, Yan S S, Dai Y Y, Zhao M W, Chen Y X, Liu G L, Mei L M, Liu Z Y and Sun J R 2010 *J. Appl. Phys.* **107** 024514
- [40] Sarkar A, Adhikari R and Das A K 2012 *Appl. Phys. Lett.* **100** 262402
- [41] Sun Z G, Miziguchi M, Manago T and Akinaga H 2004 *Appl. Phys. Lett.* **85** 5643
- [42] Mitra C, Raychaudhuri P, Dorr K, Muller K-H, Schultz L, Oppeneer P M and Wirth S 2003 *Phys. Rev. Lett.* **90** 017202, 319
- [43] Park B G et al 2011 *Nat. Mater.* **10** 347
- [44] Ramos A V, Guittet M-J, Moussy J-B, Mattana R, Deranlot C, Petroff F and Gatel C 2007 *Appl. Phys. Lett.* **91** 122107
- [45] Kang J-S et al 2008 *Phys. Rev. B* **77** 035121
- [46] Ohno H, Chiba D, Matsukura F, Omiya T, Abe E, Dietl T, Ohno Y and Ohtani K 2000 *Nature (London)* **408** 944

- [47] Moodera J S, Kinder L R, Wong T M and Meservey R 1995 Phys. Rev. Lett. 74 3273
- [48] Qu T L, Zhao Y G, Tian H F, Xiong C M and Guo S M 2007 Appl. Phys. Lett. 90 223514
- [49] A. Yanase and N. Hamada, J. Phys. Soc. Jpn. 68, 1607 (1999).
- [50] T. Nagahama, T. S. Santos, and J. S. Moodera, Phys. Rev. Lett. 99, 016602 (2007).